

# Microstructure of the hyoid bone based on micro-computed tomography findings

Xing Wang, MD<sup>a</sup>, Chaoqun Wang, MSc<sup>b</sup>, Shaojie Zhang, MSc<sup>c</sup>, Wei Wang, MD<sup>d</sup>, Xiaohe Li, PhD<sup>c</sup>, Shang Gao, PhD<sup>c</sup>, Kun Li, MSc<sup>c</sup>, Jie Chen, MSc<sup>c</sup>, Haiyan Wang, MSc<sup>c</sup>, Lianxiang Chen, PhD<sup>e</sup>, Jun Shi, PhD<sup>f</sup>, Xiaoling Liu, PhD<sup>g</sup>, Zhi-Jun Li, PhD<sup>c,\*</sup>

## Abstract

In this study, micro-CT was used to observe the microscopic anatomy of the hyoid bone, examine the variation of the trabecular bone inside the hyoid bone, and investigate the internal structure of the hyoid bone.

A total of 22 hyoid bones were scanned using micro-CT. The changes in the internal bone trabeculae were assessed with 3D reconstructions, and the fine anatomical structure of the hyoid bone was further analyzed.

Micro-CT images showed the microstructure of various parts of the hyoid bone. There were significant differences in total volume, bone volume, bone area, bone density, and volume fraction between the body and greater horns of the hyoid bone ( $P < .05$ ), but no significant differences in the ratio of bone area/volume and bone surface density were found between the body and greater horns of the hyoid bone ( $P > .05$ ). In addition, significant differences in the trabecular bone measurements, bone trabecular connectivity, and Euler number were found between the body and greater horns of the hyoid bone ( $P < .05$ ). Other parameters, including bone trabecular thickness, number of trabecular bones, bone trabecular structure model index, and anisotropy of bone trabeculae, did not differ between the body and greater horns of the hyoid bone ( $P > .05$ ). There was noticeably ossified healing at the joint between the body and greater horns of the hyoid bone.

Micro-CT can adequately display the internal structure of the hyoid bone. The identified bone structure may help clarify the physiological function of the hyoid bone. The present findings provide a theoretical basis for further studies aimed at pathological changes due to hyoid injury in clinical and forensic medicine.

**Abbreviations:** BD = bone density, BS = bone surface, BV = bone volume, DA = degree of anisotropy, Tb.N = trabecular number, Tb.Th = trabecular thickness, TV = total volume.

**Keywords:** hyoid bone, micro-CT, microstructure, quantitative analysis, trabecular bone

Editor: Michael Masoomi.

This study was supported by the National Natural Science Foundation of China (grant numbers: 81660358, 81860382, 81860383, and 81560348), Inner Mongolia Medical University Science and Technology Million Project (grant number: YKD2017KJBW009), and Inner Mongolia Natural Science Foundation (grant numbers: 2019MS08117 and 2019MS08139).

The authors have no conflicts of interest to disclose.

The datasets generated during and/or analyzed during the current study are available from the corresponding author on reasonable request.

<sup>a</sup> Beijing University of Chinese Medicine School of Traditional Chinese Medicine, Beijing, <sup>b</sup> Department of Imaging, Affiliated Hospital of Inner Mongolia Medical University, <sup>c</sup> Human Anatomy Teaching and Research Section (Digital Medical Center), Inner Mongolia Medical University Basic Medical College, <sup>d</sup> Department of Emergency, Inner Mongolia People's Hospital, <sup>e</sup> Department of Hematology, Affiliated Hospital of Inner Mongolia Medical University, Hohhot, <sup>f</sup> Department of Physiology, School of Basic Medicine, Inner Mongolia Medical University, Hohhot, Inner Mongolia, <sup>g</sup> Scientific Bureau and Department of Otolaryngology, Inner Mongolia People's Hospital, Hohhot, China.

\* Correspondence: Zhi-Jun Li, Teaching and Researching Institute of Human Anatomy, School of Basic Medicine, Inner Mongolia Medical University, 5 Xinhua St, Hohhot 010059, China (e-mail: 13904717040@qq.com).

Copyright © 2020 the Author(s). Published by Wolters Kluwer Health, Inc. This is an open access article distributed under the terms of the Creative Commons Attribution-Non Commercial License 4.0 (CCBY-NC), where it is permissible to download, share, remix, transform, and build up the work provided it is properly cited. The work cannot be used commercially without permission from the journal.

How to cite this article: Wang X, Wang C, Zhang S, Wang W, Li X, Gao S, Li K, Chen J, Wang H, Chen L, Shi J, Liu X, Li ZJ. Microstructure of the hyoid bone based on micro-computed tomography findings. *Medicine* 2020;99:44(e22246).

Received: 3 March 2020 / Received in final form: 14 July 2020 / Accepted: 18 August 2020

<http://dx.doi.org/10.1097/MD.00000000000022246>

## 1. Introduction

The hyoid bone is a unique part of the skull because it does not form joints with any other bones. The ligaments and skeletal muscles of the bones, including the humerus, mandible, thyroid cartilage, sternum, and scapula, form the supraspinatus muscles and tongue. This sub-muscle group participates in important functions, such as altering the sounds produced by the vocal cords to facilitate speech, breathing, chewing, and swallowing, and maintains the airway between the oropharynx and the tracheal ring. Most previous studies primarily focused on investigating the morphology of the hyoid bone, particularly because it relates to fractures, development of tumors, and hyoid syndrome.<sup>[1–3]</sup> However, few studies have examined the trabecular characteristics of the hyoid bone and the developmental characteristics of the ossification center between the hyoid body and the greater horns. Therefore, further studies are needed to understand the anatomical characteristics of the trabecular bone inside the hyoid bone and the function of each part of the hyoid bone.

Regular medical CT cannot clearly image the trabecular structure of the hyoid bone because of its limited resolution. Notably, micro-CT can clearly distinguish the distribution characteristics and arrangement of the intraosseous trabeculae,<sup>[4]</sup> and this high-powered image processing technology can adequately depict the microstructure inside the sample without destroying it. Micro-CT has been used in many fields, such as orthopedics and stomatology;<sup>[5–7]</sup> for instance, D'Anastasio et al<sup>[8]</sup> studied the hyoid bone of Neanderthals using micro-CT

and found that the gross anatomy of the hyoid bone of Neanderthals is almost no different from that of modern humans. The mechanical properties of the whole bone are partly controlled by the geometry of the internal trabecula and are adjusted by the corresponding forces applied to reshape the bone. However, no studies have used micro-CT to investigate the trabecular characteristics and the microstructure of the hyoid bone. The purpose of this study was to identify the characteristics and rules of trabecular changes in the hyoid bone and provide a theoretical basis for the development of the hyoid bone and the diagnosis and treatment of the hyoid bone-associated diseases. Accordingly, this study investigated the microstructures of the trabecular bone and the complete hyoid bone using micro-CT scans.

## 2. Methods

### 2.1. Specimens

Twenty-two intact hyoid bone specimens were provided by the Department of Anatomy of Inner Mongolia Medical University. The sex and age of the donors were unknown. The study was approved by the Ethics Committee of Inner Mongolia Medical University (YKD2018031)

### 2.2. Scanning methods and parameters

Extraction and characterization of the linguistic ligament were performed using micro-CT (LBF model, Hiscan XM Micro-CT; Yeeran Technology Ltd., Beijing, China) with Hiscan Analyzer Software. The scanning parameters to obtain DICOM images included the following: layer thickness=0.05 mm, layer spacing=0.05 mm, single exposure time=50 ms, bulb voltage=60 kV, current=134  $\mu$ A, matrix=2000  $\times$  1600, field of view=10 cm  $\times$  8 cm, and pixel size=0.05  $\times$  0.05 PPI. The images were acquired and stored on a Lenovo P320 workstation (Lenovo, Quarry Bay, Hong Kong) provided by Suzhou Haysfield Information Technology Co., Ltd. (Suzhou, Jiangsu, China).

### 2.3. Measurements

The following parameters were measured: total volume (TV), defined as the volume of the region of interest ( $\text{mm}^3$ ); bone volume (BV), defined as the volume of the region segmented as bone ( $\text{mm}^3$ ); bone surface (BS), defined as the surface of the region segmented as bone ( $\text{mm}^2$ ); BV fraction (BV/TV%), defined as the ratio of the segmented BV to the TV of the region of interest (ie, the ratio of BV to TV); BS density (BS/TV), defined as the ratio of the segmented BS to the TV of the region of interest ( $\text{mm}^2/\text{mm}^3$ ); specific BS (BS/BV),

defined as the ratio of the segmented BS to the segmented BV ( $\text{mm}^2/\text{mm}^3$ ); and trabecular thickness (Tb.Th), defined as the average thickness of the trabecular bone ( $\mu\text{m}$ ). Notably, in cases of osteoporosis, the Tb.Th decreases. In addition, the following parameters were also assessed: trabecular number (Tb.N), which is the number of intersections between the bone and the non-osseous tissue within a given length ( $\text{mm}^{-1}$ ); trabecular separation, the average width ( $\mu\text{m}$ ) of the medullary cavity between the trabecular bones; connectivity density, defined as a measure of the degree of connectivity of trabeculae normalized by TV ( $1/\text{mm}^3$ ), whose decline can be indicative of bone disease; structure model index, defined as an indicator of the structure of trabeculae (structure model index will be 0 for parallel plates and 3 for cylindrical rods); and degree of anisotropy (DA). In the early stages of osteoporosis, the DA of the load-bearing trabecular bone typically increases with bone mass, whereas the DA decreases when the joints loosen.<sup>[9–11]</sup> Moreover, the Euler number (Eu.N) was used to measure trabecular connectivity, with a larger number representing a greater degree of osteoporosis, and bone density (BD) was used to assess the degree of osteoporosis (Figs. 1 and 2).

### 2.4. Statistical methods

All statistical analyses were performed using SPSS 21.0 software (version 21.0; IBM, Armonk, NY). Measured data, expressed as mean  $\pm$  standard deviation ( $\bar{x} \pm s$ ), were tested for homogeneity of variance. After confirming that the relevant assumptions were satisfied, the paired t-test was used to compare the left and right hyoid angles, and the independent sample t-test was used to examine the differences between the hyoid body and the hyoid angles. A test level of  $\alpha=0.05$  was established, and a *P-value* of  $<.05$  was considered statistically significant.

## 3. Results

Micro-CT scan images of the normal hyoid bone were obtained. It was found that the body and greater horns of the hyoid bone could be divided into the intact and separated types (including the bilateral separation type and the unilateral separation type) according to the connection mode. On the Micro-CT scan images, the fine anatomical structure of the hyoid bone can be clearly shown; the bone trabeculae are mainly concentrated on both sides of the hyoid body and become thinner in the middle of the hyoid body, and those at both ends are intertwined into a network. In the greater horns of the hyoid bone, the bone trabeculae are mainly concentrated at the connection between the front end and the hyoid body. The cortex is thick, but the medullary cavity is small; the trabecular distribution is sparse.

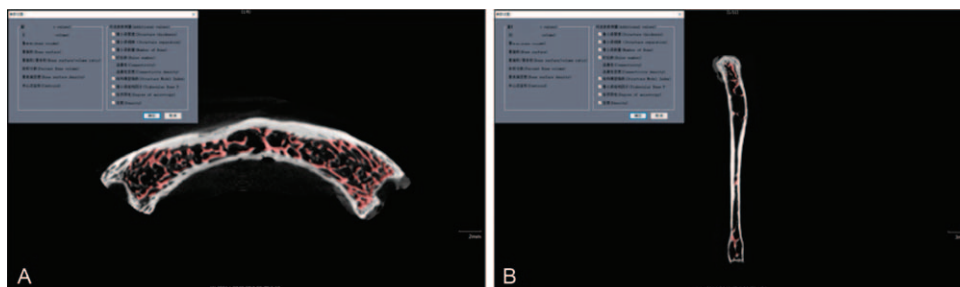


**Figure 1.** Assessment of the degree of osteoporosis in the hyoid bone. The body (A) and greater horn (B) of the hyoid bone.

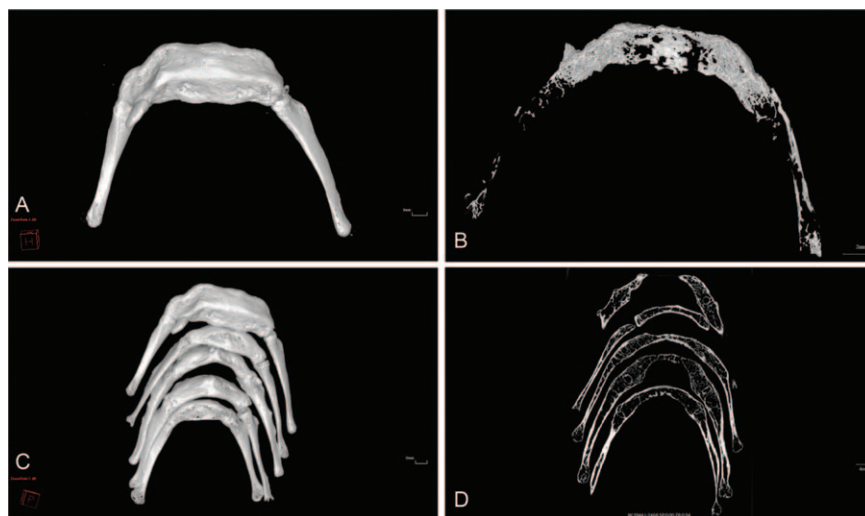


**Figure 2.** Reconstruction of the hyoid bone (A, C). Distribution characteristics and regularity of the internal trabecular bone (B, D).

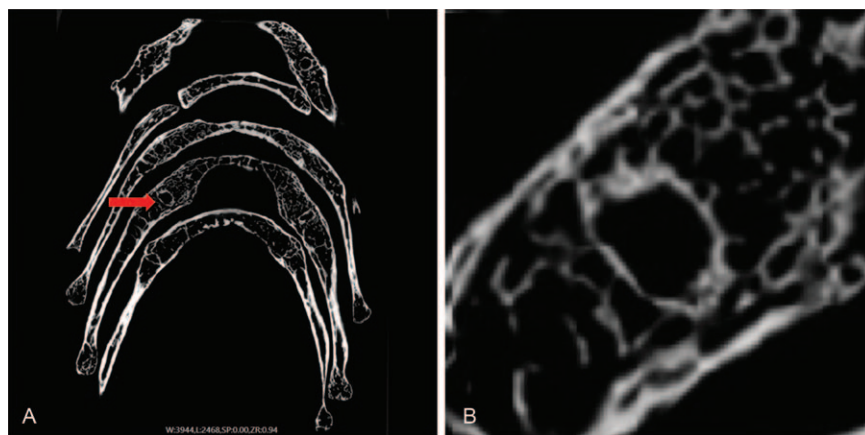


**Figure 3.** Schematic diagram of the internal ossification center of the hyoid bone at the corner joint (A). Enlarged view of the area indicated by an arrow (B).

Notably, there are obvious signs of ossification and healing at the junction between the body and greater horns of the hyoid bone (Figures 2 and 3).

There were no significant differences in the parameters between the left and right greater horns of the hyoid bone ( $P > .05$ ); therefore, these parameters were combined. TV, BV, BS, BD, and BV/TV significantly differed between the body and greater horns of the hyoid bone ( $P < .05$ ); however, no significant differences in the bone area/BV ratio and BS density were found between the body and greater horns of the hyoid bone ( $P > .05$ ; Figs. 4 and 5).

Regarding trabecula-related parameters, there were no significant differences in Tb.Th, Tb.N, structural model index, and trabecular anisotropy ( $P > .05$ ), but significant differences in Conn and Eu.N were detected between the body and greater horns of the hyoid bone ( $P < .05$ ; Table 1; Figs. 4 and 5).

#### 4. Discussion

Generally, the trabecular bone in the cancellous bone of the human body is important in supporting the hematopoietic tissue, and the direction of the trabecular bone is consistent with the

direction of the stress that the bone is subjected to. Moreover, the trabecular bone supports, cushions, and accommodates the bone marrow, as well as adapts to deformation and other functions.<sup>[12]</sup> The hyoid bone is a unique and independent “special functional bone” located in the mid-axis of the neck between the lower jaw and the small horseshoe bone between the shoulder straps. It is isolated from other joints and bone formations in the ligaments. Muscle suspension in the temporal bone styloid and mandible bone support between the throat and tongue depend primarily on the hyoid bone. In addition, these groups of muscles participate in speech, breathing, chewing, and swallowing and maintain the airway between the oropharynx and trachea ring. The hyoid bone has implications in maintaining the head posture and has a complex relationship with the mandible and cervical vertebra (Fig. 6).<sup>[13]</sup>

The hyoid bone is a whole piece of fused bone containing the main hyoid body, the large angle of the hyoid bone (greater horns), and the small “trinity” angle (lesser horns).<sup>[21]</sup> Previous morphological studies examined the hyoid bone only using naked eyes.<sup>[14,15]</sup> More recently, with the popularization of imaging technology, researchers have used radiography and CT to

**Table 1**  
Measurements of hyoid bone related indicators.

Measurement indicators	Body of the hyoid bone (22 cases)	Large angle of the hyoid bone (44 cases)	<i>t</i>	<i>P</i>
Total volume (TV; mm <sup>3</sup> )	5083.97 ± 2214.69	2923.75 ± 1404.32*	-4.70	.00
Bone volume (BV; mm <sup>3</sup> )	420.10 ± 171.56	192.33 ± 51.09*	-7.83	.00
Bone surface (BS; mm <sup>2</sup> )	2236.89 ± 893.38	1089.64 ± 305.85*	-7.41	.00
Bone density (BD; g/cm <sup>3</sup> )	1.62 ± 0.06	1.70 ± 0.76*	4.08	.00
BV/TV (%)	0.09 ± 0.02	0.07 ± 0.02*	-2.24	.03
BS/TV (mm <sup>2</sup> /mm <sup>3</sup> )	0.46 ± 0.13	0.41 ± 0.12	-1.71	.09
BS/BV (mm <sup>2</sup> /mm <sup>3</sup> )	5.52 ± 1.35	5.76 ± 1.27	0.71	.48
Trabecular thickness (Tb.Th; μm)	0.14 ± 0.01	0.15 ± 0.02	0.47	.64
Trabecular separation (Tb.Sp; μm)	0.62 ± 0.14	0.56 ± 0.13	-1.58	.12
Trabecular number (Tb.N; mm <sup>-1</sup> )	1.36 ± 0.26	1.46 ± 0.27	1.49	.14
Connectivity density (Conn.D; 1/mm <sup>3</sup> )	1250.65 ± 762.05	453.03 ± 258.71*	-6.05	.00
Structure model index(SMI)	1.42 ± 0.74	1.60 ± 0.40	1.29	.20
Degree of anisotropy (DA)	0.36 ± 0.09	0.79 ± 0.07	14.32	.00
Euler number (Eu.N)	-1249.64 ± 761.63	-451.58 ± 258.18*	6.06	.00

Tb.Sp = trabecular separation, Tb.Th = trabecular thickness.

\* denotes statistically significant relationship (*P* < .05).

observe and analyze the ossification of the hyoid bone, which is part of the endochondral bone.<sup>[16–18]</sup> Our present findings further indicate that micro-CT scanning technology can depict the shape of the hyoid bone and its internal structure. There are six ossification centers, including two in the hyoid body, two in the greater horns, and two in the lesser horns. At the end of embryonic development, the greater horns of the hyoid bone are first ossified. After birth, the hyoid body is ossified, and the ossification of the lesser horns does not happen until puberty. The hyoid bone from birth to pre-puberty is connected by a small segment of the hyoid bone and two large hyoid bones by cartilage. A pair of small horns in puberty are connected by the lingual body or the large horn. The immature hyoid bone consists of five small bones, each of which is in an ossified joint state.<sup>[19,20]</sup> Our micro-CT scans clearly showed this internal structure of the hyoid bone. The complete ossification and incomplete ossification were found between the body and the greater horns of the hyoid bone. Wang et al<sup>[22]</sup> analyzed 68 hyoid bone specimens and found that the hyoid bone was connected to the bilateral lingual bones with the large angle of the hyoid bone, and they demonstrated substantial sex differences in this region. Dong et al<sup>[23]</sup> analyzed 561 normally displayed hyoid bone CT images and divided the hyoid bone into intact and separated types

according to the image morphology (including bilateral separation and single-sided separation).<sup>[23]</sup> Using micro-CT scans, the present study observed the lingual trabecular bone in adults in the northern region in China, and our finding supports the observations by Dong et al.<sup>[23]</sup> Even within the intact hyoid bone, there was a connected ossification center at the junction of the body and the greater horns. Some of the ossification centers were completely ossified and integrated, but prolonged healing might be required despite observed healing inside the hyoid bone (Fig. 3). Some of the growth was unilateral or bilaterally separated, but not integrated. The analyses of the trabecular bone and the structure inside the hyoid bone found significant differences in the TV, BV, bone area, BD, and BV/TV between the body and the greater horns of the hyoid bone. The body of the hyoid bone was larger than the greater horns of the hyoid bone, and a part of the hyoid bone fracture was concentrated at the greater horn of the hyoid bone. In the trabecular bone, there was no significant difference in related structural parameters, such as Tb.Th, gap, and Tb.N, between the hyoid body and the greater horns of the hyoid bone, indicating that the distribution and characteristics of the trabecular bone are not obvious. The Eu.N of the trabecular bone was greater than that of the hyoid bone, and there were fewer trabecular bones at the greater horns of the

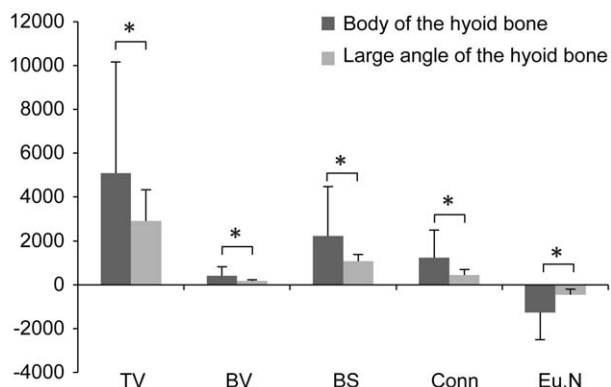


**Figure 4.** Comparison of the bone structure measurements between the body and greater horns of the hyoid bone.

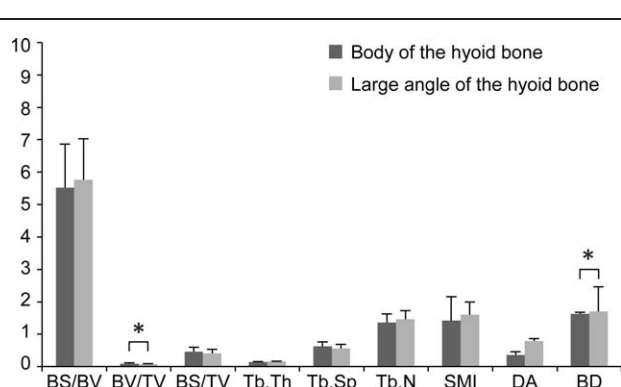


**Figure 5.** Comparison of trabecular bone-related parameters between the body and greater horns of the hyoid bone.

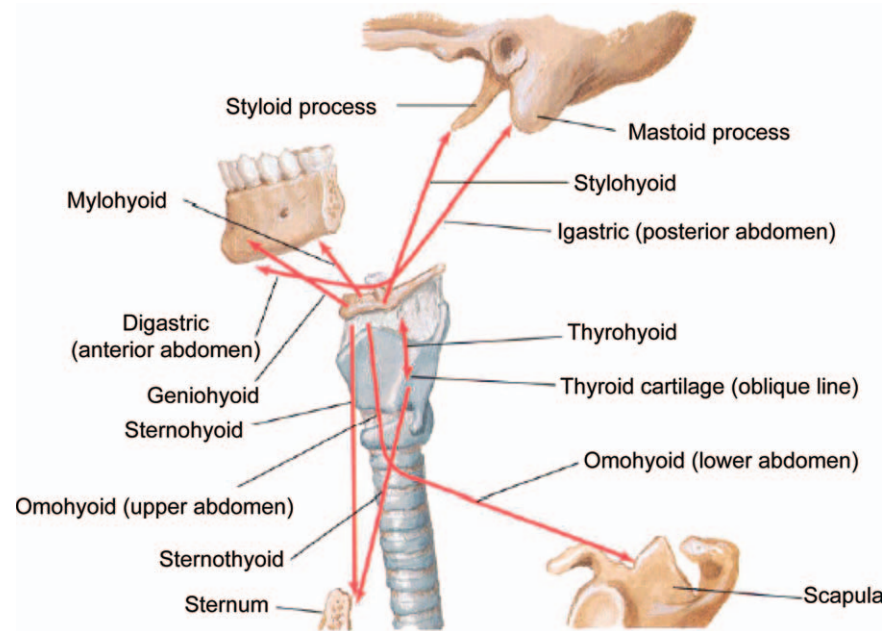


**Figure 6.** Schematic diagram of the connection between the hyoid bone and its superior and inferior muscles.

hyoid bone. Notably, in patients with head and neck cancer after radiotherapy and chemotherapy, there are changes in the trabecular bone of the hyoid bone, suggesting that radiotherapy and chemotherapy might lead to issues such as hyoid bone complications.<sup>[24]</sup>

In this study, the trabecular distribution and characteristics of the hyoid bone can be clearly observed by micro-CT, and our findings provide a certain theoretical basis for future clinical diagnosis and forensic identification. However, this study has several limitations. The sample size of the hyoid was relatively small, and the age and sex of the specimens were not clear. Therefore, further studies with a larger sample size are needed to confirm our findings and investigate age and sex-associated differences.

In conclusion, Micro-CT can adequately display the internal structure of the hyoid bone. The obtained bone structure data may help clarify the physiological function of the hyoid bone and provide a theoretical basis for further analyses aimed at pathological changes due to hyoid injury in clinical and forensic medicine.

## Acknowledgments

We thank Suzhou Haysfield Information Technology Co., Ltd. for providing specimen scanning and data analysis for this study. We also would like to thank Editage (www.editage.cn) for English language editing.

## Author contributions

XXXX.

## References

- [1] Porr J, Laframboise M, Kazemi M. Traumatic hyoid bone fracture - a case report and review of the literature. *J Can Chiropr Assoc* 2012;56:269–74.
- [2] Sychra V, Eßer D, Kosmehl H, et al. Unusual manifestation of a multiple myeloma in the hyoid bone. *Dentomaxillofac Radiol* 2013;42:27101530.
- [3] Gnanadev R, Iwanaga J, Loukas M, et al. An unusual finding of the hyoid bone. *Cureus* 2018;10:e3365.
- [4] Feldkamp LA, Goldstein SA, Parfitt AM, et al. The direct examination of three-dimensional bone architecture in vitro by computed tomography. *J Bone Miner Res* 1989;4:3–11.
- [5] Baltacıoğlu İH, Demirel G, Kolsuz ME, et al. In-vitro analysis of maxillary first molars morphology using three dimensional Micro-CT imaging: considerations for restorative dentistry. *Eur Oral Res* 2018;52:75–81.
- [6] Xu Y, Meng H, Yin H, et al. Quantifying the degradation of degradable implants and bone formation in the femoral condyle using micro-CT 3D reconstruction. *Exp Ther Med* 2018;15:93–102.
- [7] Moncayo-Donoso M, Guevara JM, Márquez-Flórez K, et al. Morphological changes of physal cartilage and secondary ossification centres in the developing femur of the house mouse (*Mus musculus*): a micro-CT based study. *Anat Histol Embryol* 2019;48:117–24.
- [8] D'Anastasio R, Wroe S, Tuniz C, et al. Micro-biomechanics of the Kebara 2 hyoid and its implications for speech in Neanderthals. *Plos One* 2013;8:e82261.
- [9] Chen H, Zhou X, Fujita H, et al. Age-related changes in trabecular and cortical bone microstructure. *Int J Endocrinol* 2013;2013:213234.
- [10] Agarwal SC, Dumitriu M, Tomlinson GA, et al. Medieval trabecular bone architecture: the influence of age, sex, and lifestyle. *Am J Phys Anthropol* 2004;124:33–44.
- [11] Green JO, Nagaraja S, Diab T, et al. Age-related changes in human trabecular bone: relationship between microstructural stress and strain and damage morphology. *J Biomech* 2011;44:2279–85.
- [12] Wolf J. *Das Gesetz der Transformation der Knochen*[M]. Berlin: Hirschwald 1892;11–13.
- [13] Auvenshine RC, Pettit NJ. The hyoid bone: an overview. *Cranio* 2020;38:6–14.
- [14] O'Halloran RL, Lundy JK. Age and ossification of the hyoid bone: forensic implications. *J Forensic Sci* 1987;32:1655–9.
- [15] Kim DI, Lee UY, Park DK, et al. Morphometrics of the hyoid bone for human sex determination from digital photographs. *J Forensic Sci* 2006;51:979–84.
- [16] Fakhry N, Puymerail L, Michel J, et al. Analysis of hyoid bone using 3D geometric morphometrics: an anatomical study and discussion of potential clinical implications. *Dysphagia* 2013;28:435–45.

- [17] Fisher E, Austin D, Werner HM, et al. Hyoid bone fusion and bone density across the lifespan: prediction of age and sex. *Forensic Sci Med Pathol* 2016;12:146–57.
- [18] Tamimi D, Hatcher D. *Specialty Imaging: Temporomandibular Joint*. Philadelphia, PA: Elsevier.
- [19] Chaoyou Z. *Human Anatomy* (volume 1). Beijing: People's Medical Publishing House.
- [20] Moore K, Dalley A, Agur A. *Clinically Oriented Anatomy*. Baltimore, MD: Lippincott Williams & Wilkins.
- [21] Wenlong D, Liu X. *Systemic Anatomy*. Beijing: People's Medical Publishing House.
- [22] Wang J, Chen LS, Lu SX, et al. Morphological characteristics of hyoid bone and its gender difference. *Fa Yi Xue Za Zhi* 2013;29:176–9.
- [23] Dong X, Liu JP, Zhi JX, et al. CT study of hyoid bone morphology. *J Clin Radiol* 2001;20:723–4.
- [24] Hatakeyama H, Fujima N, Tsuchiya K, et al. Osteoradionecrosis of the hyoid bone after intra-arterial chemoradiotherapy for oropharyngeal cancer: MR imaging findings. *Cancer Imaging* 2017;17:22.